Transcriptome profiling reveals Silibinin dose-dependent response network in non-small lung cancer cells

Jagan Mohan Kaipa[1,2,3], Vytaute Starkuviene[2,4], Holger Erfle[2], Roland Eils[5,6] and Evgeny Gladilin[2,7,8]

[1] Helmholtz Center for Infection Research, Braunschweig, Germany
[2] BioQuant, University Heidelberg, Heidelberg, Germany
[3] Theoretical Bioinformatics, German Cancer Research Center, Heidelberg, Germany
[4] Institute of Biosciences, Vilnius University Life Science Center, Vilnius, Lithuania
[5] Center for Digital Health, Berlin Institute of Health and Charité Universitätsmedizin Berlin, Berlin, Germany
[6] Health Data Science Unit, Heidelberg University Hospital, Heidelberg, Germany
[7] Leibniz Institute of Plant Genetics and Crop Plant Research, Seeland, Germany
[8] Applied Bioinformatics, German Cancer Research Center, Heidelberg, Germany

ABSTRACT

Silibinin (SIL), a natural flavonolignan from the milk thistle (Silybum marianum), is known to exhibit remarkable hepatoprotective, antineoplastic and EMT inhibiting effects in different cancer cells by targeting multiple molecular targets and pathways. However, the predominant majority of previous studies investigated effects of this phytocompound in a one particular cell line. Here, we carry out a systematic analysis of dose-dependent viability response to SIL in five non-small cell lung cancer (NSCLC) lines that gradually differ with respect to their intrinsic EMT stage. By correlating gene expression profiles of NSCLC cell lines with the pattern of their SIL IC50 response, a group of cell cycle, survival and stress responsive genes, including some prominent targets of STAT3 (BIRC5, FOXM1, BRCA1), was identified. The relevancy of these computationally selected genes to SIL viability response of NSCLC cells was confirmed by the transient knockdown test. In contrast to other EMT-inhibiting compounds, no correlation between the SIL IC50 and the intrinsic EMT stage of NSCLC cells was observed. Our experimental results show that SIL viability response of differently constituted NSCLC cells is linked to a subnetwork of tightly interconnected genes whose transcriptomic pattern can be used as a benchmark for assessment of individual SIL sensitivity instead of the conventional EMT signature. Insights gained in this study pave the way for optimization of customized adjuvant therapy of malignancies using Silibinin.

Subjects Bioinformatics, Cell Biology, Genetics, Drugs and Devices, Oncology
Keywords Silibinin, Custom drug response, Adjuvant cancer therapy, Transcriptome profiling, Drug susceptibility network

Submitted 8 July 2020
Accepted 26 October 2020
Published 16 December 2020

Corresponding author
Evgeny Gladilin,
evgeny.gladilin@gmail.com

Academic editor
Vladimir Uversky

Additional Information and Declarations can be found on page 16

DOI **10.7717/peerj.10373**

INTRODUCTION

The ability of malignant cells to attain drug resistance and to escape cell death frequently observed in different types of cancer represents the major challenge to chemical tumor therapy. Several evolutionary conserved mechanisms mediate elevated survival capabilities

and drug resistance of cancer cells including inhibition of apoptotic pathways, alteration and enhancement of metabolism, DNA damage repair, drug inactivation or alteration, genetic and epigenetic activation of stress response and proliferation programs such as epithelial-mesenchymal transition (EMT) (*Michael & Doherty, 2005*; *Hang, Cai & Fan, 2013*; *Housman et al., 2014*; *Hanahan & Weinberg, 2011*). As a consequence of elevated environmental adaptation and self-reprogramming capabilities, cancer cells often attain resistance against targeted drugs and even drug combinations by bypassing affected pathways (*Patel & Rothenberg, 1994*; *Clarke et al., 2019*). In most of the tumors, multiple survival mechanisms and pathways are active in parallel. A network of dozens tightly interconnected genes rather than just few linear signaling pathways maintain abnormal survival and resistance capabilities of cancer cells (*Gladilin & Eils, 2017*).

A promising approach to overcome the limitations of conventional therapy is a combination of targeted and sensitizing drugs (*Chandarlapaty et al., 2010*; *Al-Lazikani, Banerji & Workman, 2012*). In view of often unavoidable side effects of targeted therapy, sensitizing compounds with a low toxicity for healthy cells are preferred that are still capable to weaken abnormally functioning tumor cells. There is an increasing body of evidence that secondary plant metabolytes such as various polyphenolic compounds exhibit distinctive antineoplastic properties that make them promising sensitizing agents for combined tumor therapy (*Gerhäuser, 2012*; *Wang et al., 2016*; *Dayem et al., 2016*; *Thomford et al., 2018*). Some of these natural compounds have a long history of usage as nutrition supplements in traditional medicine, and were empirically proven to be well tolerated.

One of the antineoplastic phytocompounds increasingly gaining attention in the last two decades is Silibinin (also known as Silybin or Silymarin)—a flavonolignan from the milk thistle *Silybum marianum*. Silibinin is a mixture of two diastereoisomers Silybin A and Silybin B, at a ratio of 1:1 (*Agarwal et al., 2003*). Originally known as a hepatoprotective dietary drug (*Machicao & Sonnenbichler, 1977*; *Sonnenbichler et al., 1999*; *Flora et al., 1998*; *Vargas-Mendoza, 2014*; *Hellerbrand et al., 2016*), in recent years Silibinin has been shown to exhibit remarkable antineoplastic properties crossover different types of tumors which was attributed to different molecular mechanisms and signaling pathways (*Fraschini, Demartini & Esposti, 2002*; *Gazak, Walterova & Kren, 2007*; *Ramasamy & Agarwal, 2008*; *Ting, Deep & Agarwal, 2013*; *Polachi et al., 2016*). Meanwhile more than 1,500 studies on hepatoprotective and antineoplastic effects of Silibinin and their mechanisms in different tissues and cells were published (*Pubmed, 2019*). The predominant majority of these works were, however, performed with one particular cell line and typically focused on a few molecular targets and signaling/metabolic pathways directly or indirectly affected by Silibinin, see Table 1. Primary molecular targets and mechanisms of SIL action in particular type of cancer tissue/cells were usually hypothesized and rarely investigated mechanistically. As direct molecular binding targets of Silibinin several drivers and mediators of malignant transformation were reported, see Table 2.

As a multitarget compound with a broad spectrum of antineoplastic action Silibinin combines the ability to selectively reduce viability of cancer cells in a dose dependent manner (*Katiyar, Roy & Baliga, 2005*; *Mokhtari, Motamed & Shokrgozar, 2008*; *Zhan et al., 2011*; *Su et al., 2013*; *Wang et al., 2014b*) with low toxicity for normal tissues even in the range of

Table 1 Overview of studies on antineoplastic effects of Silibinin in different cancer tissues/cells.

Cancer tissue, cell type	Molecular mechanisms	Lit.
H. lymphoma, U-937	Inh: TNF, NF-kB, MAPK8	*Manna et al. (1999)*
H. colon cancer, HT-29	Up: p27, p21	*Agarwal et al. (2003)*
	Down: CCNE1, CCND1, CDC25C, CCNB1	
	Inh: CDK2, CDK4, CDC2	
M. SKH-1 epidermis	Up: p53, p21	*Dhanalakshmi et al. (2004)*
H. endothelium, ECV304	Up: Bax	*Yoo et al. (2004)*
	Down: Bcl-2	
	Inh: NF-kB	
	Act: CASP3, CASP9	
M. keratinocytes, JB6 C141	Up: p53, Bax, CYCS	*Katiyar, Roy & Baliga (2005)*
	Down: Bcl-2	
	Act: CASP3, APAF1, PARP-1	
H. colorectal cancer, SW480	Inh: PIK3CA-Akt-mTOR	*Raina et al. (2013)*
	Act: MAP2K1/2-MAPK1/3	
H. breast cancer, MCF-7	Inh: HSP90	*Zhao et al. (2011)*
H. lung cancer, A549	Inh: PI3K-Akt-MAPK	*Chen et al. (2005)*
H. breast cancer, MCF-7, MDA-MB-231	Inh: Notch-1	*Kim et al. (2014b)*
	Down: ERK, Akt, AIF, CASP3	
H. lung cancer	Inh: EGFR	*Hou et al. (2018)*
H. colorectal adenocarcinoma, LoVo	Inh: GLUT1	*Catanzaro et al. (2018)*
H. glioblastoma, A172, SR	Inh: mTor, Yap	*Bai et al. (2018)*
H. prostate cancer, DU145, PC3	Up: p27, p21	*Davis-Searles et al. (2005)* *Deep et al. (2006)*, *Mokhtari, Motamed & Shokrgozar (2008)*
	Down: CDK4, CDK6, CDK2, CCNE1, CCND1, CCNB1	
H. umbilical vein endothelial cells, HUVEC	Inh: NF-kB	*Kang et al. (2003)*
	Down: VCAM-1, ICAM-1, CD62E	
H. lung cancer, PC-9	Up: CDH1	*Cufí et al. (2013)*
	Down: VIM	
H. bladder cancer, T24	Inh: CTNNB1/ZEB1	*Wu et al. (2013)*
H. breast cancer, MDA-MB-231	Inh: CXCR4	*Wang et al. (2014a)*
H. breast cancer, MDA-MB-231	Down: CDC42, D4-GDI	*Dastpeyman et al. (2012)*
H. leukemia, THP-1	Inh: p65, ICAM-I	*Chen et al. (2014)*
H. lung cancer, A549	Inh: STAT1, STAT3, NF-kB	*Chittezhath et al. (2008)*
H. cervical cancer, HeLa; H. hepatoma, Hep3B	Inh: STAT1, STAT3, NF-kB	*García-Maceira & Mateo (2009)*
H. breast cancer, MCF7	Up: BNIP3	*Jiang et al. (2015)*
H. prostate cancer, PCA	Down: SREBP1/2	*Nambiar et al. (2014)*
	Up: AMPK	
H. prostate cancer, LNCaP	Up: p21, p27	*Zi & Agarwal (1999)*

(*continued on next page*)

Table 1 (*continued*)

Cancer tissue, cell type	Molecular mechanisms	Lit.
	Down: CCND1, CDK4, CDK6	
H. colon cancer	Up: Bax	*Kauntz et al. (2012)*
	Down: Bcl-2, IL1β, TNFα, MMP7	
H. colon cancer, SW480	Act: CASP3, CASP8	*Kauntz (2012)*
H. lung cancer, H1975, HCC827, A549, H460, H1299	Inh: EGFR, LOX	*Hou et al. (2018)*
H. lung cancer	Down: HIF1A, TNFα, NK-kB, STAT3	*Tyagi et al. (2009)*
	Up: Ang-2, Tie-2, TIMP-1, TIMP-2	
H. cervical cancer, HeLa	Up: ROS, NOS	*Fan et al. (2011)*
H. lung cancer, MCF-7	Down: Er α, mTor, ERK	*Zheng et al. (2015)*
H. glioma, U87, U251	Down: PI3K, FOXM1	*Zhang et al. (2015)*
H. breast cancer, MCF7	Down: Bcl-2, BRCA1	*Pirouzpanah et al. (2015)*
H. colon cancer, HCT116	Inh: CD44v6	*Patel et al. (2018)*
	Down: Nanog, CTNNB1, CDKN2A	
	Up: CDH1	
H. prostate cancer, DU145	Inh: STAT3, pSTAT3	*Agarwal et al. (2007)*
H. gastric cancer, MGC803	Inh: STAT3, pSTAT3	*Wang et al. (2014b)*
H. pancreatic cancer, S2-013, T3M4, HEK-293T	Inh: STAT3, pSTAT3, c-Myc	*Shukla et al. (2015)*
H. breast cancer, MDA-MB468, BT20	Inh: STAT3	*Kim et al. (2014a)*
H. breast cancer, MDA-MB-231	Inh: STAT3	*Byun et al. (2017)*

Notes.
Abbreviations: Up, upregulation; Down, downregulation; Inh, inhibition; Act, activation; H, human; M, mice.

Table 2 **Overview of reported direct molecular binding targets of Silibinin.**

Protein name	Gene symbol	Lit.
Cytochrom P450 2C9	CYP2C9	*Beckmann-Knopp et al. (2000)*, *Kawaguchi-Suzuki et al. (2014)* *Bijak (2017)*, *Por et al. (2018)*
CXC-Motiv-Chemokinrezeptor 4	CXCR4	*Wang et al. (2014a)*
Mitogen-Activated Protein Kinase 11	MAPK11	*Youn et al. (2013)*
G-protein coupled receptor 12	GPR120	*Chinthakunta et al. (2018)*
Cyclooxygenase-2	COX-2	*Malik, Manan & Kirza (2017)*
Phospholipase A2	PLA2	*Malik, Manan & Kirza (2017)*
Aldo-Keto Reductase Family 1 Member D1	AKR1D1	*Malik, Manan & Kirza (2017)*
Core 1 β1,3-galactosyltransferase	C1GALT1	*Lin et al. (2018)*
β-catenin	CTNB1	*Iftikhar & Rashid (2014)*
Epidermal Growth Factor Receptor	EGFR	*Hosen et al. (2016)*
Heat Shock Protein 90	HSP90	*Zhao et al. (2011)*, *Riebold et al. (2015)*, *Cuys et al. (2019)*
Signal Transducers and Activators of Transcription 3	STAT3	*Bosch-Barrera & Menendez (2015)*, *Bosch-Barrera, Queralt & Menedez (2017)* *Verdura et al. (2018)*, *Qin et al. (2019)*

high, therapeutically relevant doses of more than 1,500 mg/day (*Soleimani et al., 2019*). However, the knowledge of primary targets alone does not provide yet a reliable criterion for quantitative assessment of SIL efficiency in application to a particular cancer tissue/cell. One of the global factors known to be relevant to the drug dose response is the intrinsic EMT stage of cancer cells. Accordingly, cells exhibiting mesenchymal pheno-/genotypic profiles are more drug-resistant to antineoplastic drugs than epithelial cells (*Tan et al., 2014*). It is, however, not known whether this rule also applies to Silibinin. Here, we address this question by a systematic analysis of dose-dependent viability response to SIL in five non-small cell lung cancer (NSCLC) lines (H1650, H1975, A549, H838, H2030) that gradually differ with respect to their intrinsic EMT stage defined by the transcriptomic signature from (*Byers et al., 2013*). The relationship between SIL IC50 viability response and gene expression profiles of five NSCLC cell lines was compared with a reference compound, Withaferin-A, which is known to exhibit dose-dependent EMT-inhibiting effects (*Vanden Berghe et al., 2012*; *Vyas & Singh, 2014*; *Gladilin, Gonzalez & Eils, 2014*). Our experimental results show that in contrast to WFA SIL does not exhibit a EMT-conform dose–response. Instead, SIL viability response of NSCLC cells turns out to correlate with the expression level of cell cycle, survival and stress responsive genes including some prominent targets of *STAT3*.

MATERIALS AND METHODS

Cell culturing

Human lung adenocarcinoma cell lines H1650, H1975, A549, H838, H2030 were obtained from ATCC and cultured in DMEM (Dulbecco's Modified Eagle Medium) medium supplemented with 10% fetal calf serum (FCS) and 100 U/ml penicillin G and 100 µg/ml streptomycin sulfate at 37 °C in a humidified 5%CO_2 incubator. To ensure the ample number of cell count, cells were cultured three days prior to cell seeding. When the culture plates became confluent, NSCLC cells were detached and collected in a sterile Falcon tube with a pre-warmed medium for transfection. Cells were subjected to centrifugation (at 1000 rpm and room temperature for 5 min) and the supernatant was aspirated. The cells were resuspended in the medium for transfection. The number of cells/ml was determined by using Neubauer counting chamber and cells were diluted to get a concentration of 12000 cells/100 µl of the medium. After careful optimization of transfection efficiency, 12000 cells/well in 100 µl was found to show good transfection rate.

Silibinin and Withaferin-A compounds

Silibinin ($C_{25}H_{22}O_{10}$, mol. weight 482.44) and Withaferin-A ($C_{28}H_{38}O_{6}$, mol. weight 470.60) both were purchased from Sigma-Aldrich (Germany). Both compounds were dissolved in dimethylsulfoxide (DMSO; Sigma-Aldrich) to make a stock solution. The final concentration of DMSO in the culture medium did not exceed 0.5% which has no detectable effects on cells.

CellTiter-Blue cell viability assay

Cells seeded into 96-well plates in sextuplicate at a density of 15×10^3 cells per well. Twenty-four hours after seeding, the cells were treated with various concentrations of

Withaferin-A and Silibinin for totally 24 h. To measure the viability of cells, CellTiter-Blue® Viability Assay (Promega, G8081) was applied according to the manufacturer's instructions. Incubation with the dye for 60 min was followed by measurement of the fluorescence with the infinite F200 pro Reader (TECAN). A blank well without cells was measured to determine the background. After subtraction of the background, cell dilution series enabled due to a direct correlation of the signal intensities with the cell number, the verification of absolute cell numbers.

Determination of IC50 from CTB measurements

The half maximal inhibitory concentration (IC50) was determined from series of dose-dependent CTB measurements using following basic steps. First, the raw CTB intensity measurements (I_i) were normalized by the intensity level (I_0) of the reference (untreated) probe:

$$nI_i = 100\frac{I_i}{I_0}. \tag{1}$$

Subsequently, the average pattern of normalized dose response (anI_i) from N different measurements was calculated:

$$anI_i = \frac{1}{N}\sum_{j=1..N} nI_i(j). \tag{2}$$

Finally, the IC50 value of a particular cell line and measurement condition (e.g., duration of treatment) was determined from the average normalized pattern of IC50 dose response by fitting the Hill's sigmoid function (*Spiess & Neumeyer, 2010*; *Sebaugh, 2011*)

$$anI(D) = \min + \frac{\max - \min}{1 + (\frac{D}{IC50})^H}, \tag{3}$$

where D is the drug dose, min and max are the minimum and maximum values of anI, $IC50$ and H are the IC50 and the Hill's coefficient values that are determined from the fit. The nonlinear least square fit of the Hill's equations was performed automatically using the MATLAB R2019b (The Mathworks, Inc.). To characterize relative differences in viability response (V_i) among five NSCLC cell lines ($i = 1..5$), normalized IC50 values (nV_i)

$$nV_i = \frac{V_i - V_{\min}}{V_{\max} - V_{\min}} \in [0, 1] \tag{4}$$

and their ranks (R_i)

$$R_i = \text{rank}(V_i, [V_1, V_2, V_3, V_3, V_4, V_5]). \tag{5}$$

were calculated.

Determination of total cell count using quantitative image analysis

Quantitative image analysis was performed to acquire the total cell count. Immediately after the measurement of the fluorescence signal, the medium is aspirated from 96well plate containing NSCLC cells and washed with PBS solution twice to ensure the complete removal of dead cells. Since dead cells do not attach to the surface and freely float in the

medium, washing twice with PBS removes approximately all the dead cells from the well. After washing, 70 µl cell fixation solution (PFA 3% + Hoechst dye) was added to each well for the fixation and nuclei staining of cells by a single step. Cells were incubated at 4 °C for 48 h. Wells were washed with PBS twice after incubation to remove unbound Hoechst dye and analyzed under a microscope (Olympus FV 3000) for counting the stained nuclei. Finally, the cell counting was performed manually with the help of images obtained from the microscope.

In vitro cell migration assay

For measurement of cell motility, 2D cell migration assay from (*Marwitz et al., 2016*) was used. Cells were seeded in 24-well plate (Zell Kontakt 3231-20) at a density of 2,000–5,000 cells/well (depends from cell lines). Twenty-four hours after seeding the cells were treated with various concentrations of Withaferin-A and Silibinin for a total of 24 h and after stained with Hoechst (Sigma) for 1 h. Images were acquired in 20 min intervals for 48 h using environment-controlled microscope (IX81, Olympus) equipped with an UPlanSApo 10 × /0.4 objective lens (Olympus). Nine positions per well (3 × 3 grid) were imaged and stitched with a ImageJ plugin (*Preibisch, Saalfeld & Tomancak, 2009*). Single cell tracking was performed with ImageJ Mtrack2 plugin. Speed of each tracked cell was calculated by dividing total travelled distance by total time, for which cell was tracked. Persistence was calculated by dividing the distance between the first and the last point, where the cell was tracked, by total travelled distance. Resulting number was multiplied by the square root of time, for which cell was tracked divided by maximal possible tracking time, in order to penalize cells, which were tracked for a shorter period of time.

Immunofluorescence and microscopic imaging

Cells were fixed for 5 min in 3.7% PFA in PBS at RT, permeabilized with ice-cold 0.1% TritonX-100 in PBS for 5 min, blocked for 30 min with Blocking solution (3% BSA, 2.5% FCS) and stained with primary antibodies to vimentin and actin (Abcam, Cambridge, UK) for 1 h. After staying cells were washed 3 times in PBS and stained with secondary antibodies, Phalloidin-BODIBY (Thermo Fisher) and Hoechst (Sigma) for 30 min. Imaging was performed using the confocal laser scanning microscope (Olympus FV 3000) with 64x oil immersion lens to visualize the actin and vimentin network as well as the nucleus in the cells.

Gene expression data

Gene expression (GE) data of H1650, H1975, A549, H838, H2030 cell lines from GSE47206 (*El-Chaar et al., 2014*) were used for computational analysis of correlation between transcriptomic and IC50 profiles of NSCLC cells. Analysis was performed only for transcripts with the detection significance of $p < 0.05$ (P,M) in all five NSCLC cell lines. Trancripts with the non-significant level of detection (A) were excluded from analysis.

GO enrichment analysis

Gene ontology enrichment analysis was performed using STRING v11 (*Szklarczyk et al., 2019*) with the significance level of $p < 0.05$ after multiple testing correction (*Benyamini & Hochberg, 1995*) for each functional classification framework (GO, KEGG, InterPro, etc.).

Table 3 List of siRNAs used for protein knockdown by gene silencing.

Gene	Full Name	Sense siRNA Sequence	Antisense siRNA Sequence
BIRC5	Baculoviral IAP repeat containing 5	GGACCACCGCAUCUCUACATT	UGUAGAGAUGCGGUGGUCCTT
BIRC5	Baculoviral IAP repeat containing 5	GCAGGUUCCUUAUCUGUCATT	UGACAGAUAAGGAACCUGCAG
BIRC5	Baculoviral IAP repeat containing 5	CAAAGGAAACCAACAAUAATT	UUAUUGUUGGUUUCCUUUGCA
FOXM1	Forkhead box M1	GCUCAUACCUGGUACCUAUTT	AUAGGUACCAGGUAUGAGCTG
FOXM1	Forkhead box M1	CACUAUCAACAAUAGCCUATT	UAGGCUAUUGUUGAUAGUGCA
FOXM1	Forkhead box M1	GGAUCAAGAUUAUUAACCATT	UGGUUAAUAAUCUUGAUCCCA
BRCA1	Breast cancer 1, early onset	GGGAUACCAUGCAACAUAATT	UUAUGUUGCAUGGUAUCCCTC
BRCA1	Breast cancer 1, early onset	CAGCUACCCUUCCAUCAUATT	UAUGAUGGAAGGGUAGCUGTT
BRCA1	Breast cancer 1, early onset	CAUGCAACAUAACCUGAUATT	UAUCAGGUUAUGUUGCAUGGT

Transfection of NSCLC cells

All siRNA used for knockdown of *BIRC5*, *FOXM1*, *BRCA1* was purchased from Ambion®ThermoFisher Scientific, see Table 3.

Transfection experiments were carried out by lipofection technique using Lipofectamine®2000 (Invitrogen), with transient expression. Two types of transfection methods were performed in the optimization of transfection efficiency: reverse and forward transfection.

Forward and reverse transfection method

Forward transfection is a conventional method of transfection where cells are first seeded for 24 h and stored at 37 °C and 5% CO_2. After incubation, cells are transfected as per company's (Invitrogen) protocol. In reverse transfection, unlike conventional transfection, the genetic material is coated on the bottom of well plates prior to the seeding of NSCLC cells into multi-well plate. As the order of adding genetic material is reverse compared to the conventional method it is named as reverse transfection method. Multi-well plates are coated with required siRNA to be transfected along with gelatin, fibronectin and transfection reagent (Lipofectamine®2000) stored at 4 °C for 28 h and stored in dry place. Later, NSCLC cells were seeded into these wells, incubated for 28 h to attain transfected cells.

Detection of siRNA mediated gene silencing

Estimation of transfection efficiency of the NSCLC cells was performed by blocking PLK1 (polo-like-kinase-1) enzyme using RNA silencing technique via small interfering RNA (siRNA). Expression of PLK1 has several functions like the initiation of mitosis, cytoplasmic separation, mitotic spindle formation and membrane formation in telophase of mitosis by phosphorylating mitotic kinesin-like protein-1. Silencing of PLK1 leads to mitotic cell arrest and the centrosomes lose the ability to nucleate microtubules. This effect can be observed under a microscope with star shape nuclear phenotype. Presence of star shape nucleus indicates that the PLK1 was successfully silenced that in turn confirms that the cells are transfectable.

Immunoblotting

The confirmation of knockdown efficiency was carried out using Western Blot analysis. Harvesting and samples for analysis were prepared by removing supernatant from the cells followed by addition of 500 µl of PBS. Cells were resuspended and transferred to 1.5 ml for centrifugation for 5 min at 1,600 RPM. After centrifugation, PBS was removed without disturbing cell pellet. 25 µl of 1x Laemlli buffer containing DTT (final concentration 100 mM) was added and incubated for 10 min at 95 °C. Proteins in the sample were separated by SDS-PAGE in a 10% resolving gel and transferred onto methanol-activated PVDF membranes by semi-dry blotting technique using transfer buffer at a constant current of 130 V until the sample reaches the resolving gel. As soon as the sample reaches resolving gel electrophoresis is run at 90V. The membrane was blocked with 5% milk powder, 0.5% BSA in PBST for 1 h at room temperature. After blocking, the membrane was incubated with specific primary antibody in 5% (w/v) milk powder/PBST overnight at 4 °C. To remove the unbound primary antibody three subsequent washings for 10 min with PBST were performed. Then the membrane was incubated with the horseradish peroxidase (HRP) coupled secondary antibody in 5% (w/v) milk powder, 0.5% BSA in PBST for 1 h at room temperature. Three subsequent PBST washing were performed to ensure complete removal of the secondary antibody. Detection of proteins was carried out by using ECL chemiluminescent immunodetection system with different exposure time using INTAS Fluoreszenz u. ECL Imager. Subsequently, quantitative analysis of Western Blot images was performed using ImageJ according to a standard protocol (http://www.openwetware.org/wiki/Protein_Quantification_Using_ImageJ). Figure S5 shows exemplary analysis of transient knockdown of target proteins *FOXM1* and *BIRC5* in A549 and H838 NSCLC cells using small-interfering RNA (siRNA) vs β-actin as a loading control.

RESULTS

The intrinsic EMT stage of NSCLC cell lines was ranked according to the expression level of E-cadherin (*CDH1*) as suggested by *Byers et al. (2013)*, see Table S1. Accordingly, five NSCLC cell lines (H1650, H1975, A549, H838, H2030) exhibit gradual difference in their intrinsic EMT stage: from most epithelial (H1650) to most mesenchymal (H2030), respectively.

Dose-dependent response of all five NSCLC cell lines to 24 h, 48 h and 72 h exposure with Silibinin (SIL) and the reference compound, Withaferin-A (WFA), measured via the CellTiter-Blue® Cell Viability Assay was used to determine IC50 values of both compounds. Figure 1 shows dose response curves and SIL/WFA IC50 values of all five NSCLC cell lines.

As one can see from the overview of SIL/WFA IC50 ranks of all five NSCLC cell lines in Fig. 2, the pattern of WFA IC50 values exhibits a strong correlation with the intrinsic EMT stage of NSCLC cells, while SIL IC50 does not show such a correlation. Strikingly, all cell lines with exception of H838 have a comparable level of SIL IC50.

To test possible dependency of the drug response on the intrinsic EMT stage of NSCLC cells, Spearman (rank) correlation between the pattern of normalized SIL and WFA IC50

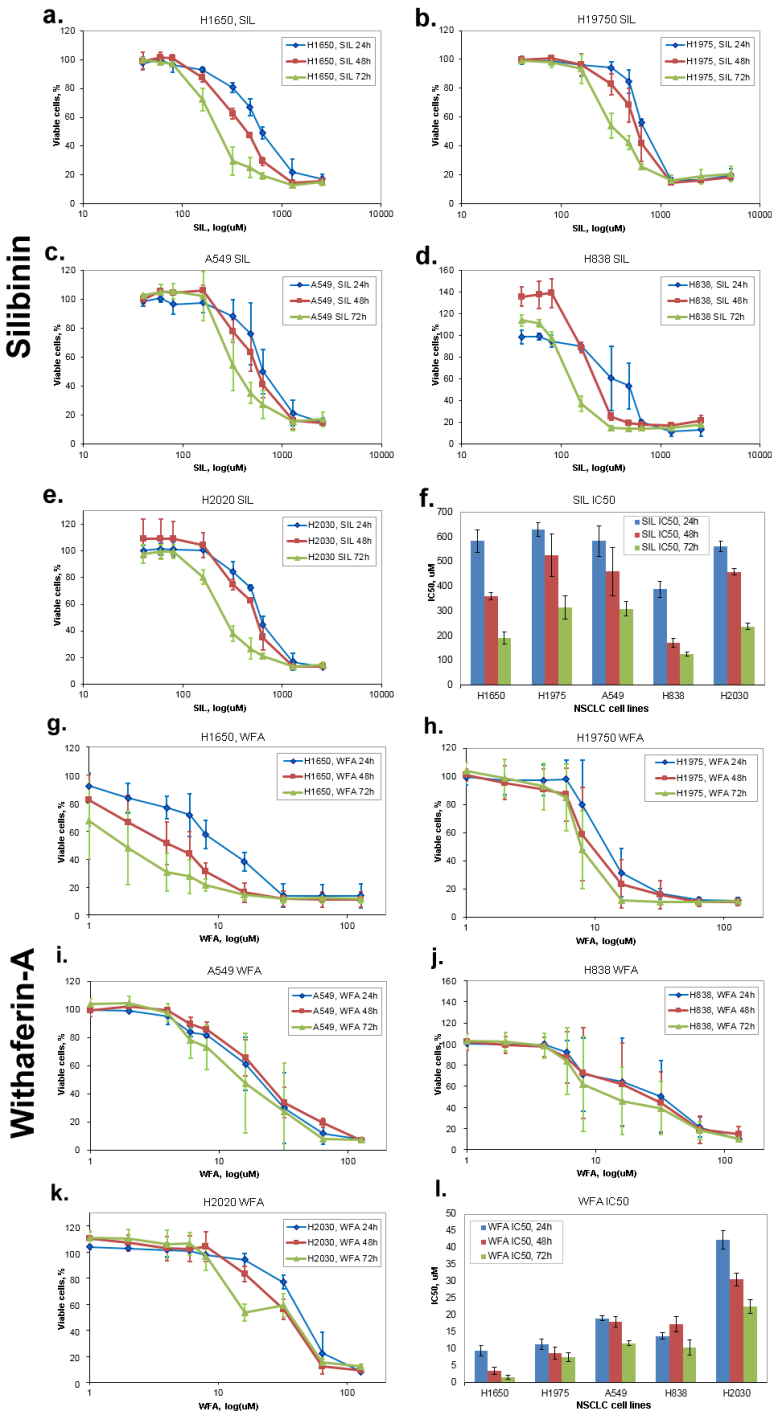

Figure 1 Dose-dependent 24 h, 48 h, 72 h response of NSCLC cells lines to Silibinin (A–F) and Withaferin-A (G–L): (A, G) H1650, (B, H) H1975, (C, I) A549, (D, J) H838, (E, K) H2030, (F, L) mean SIL IC50 values for all five NSCLC cell lines. Error bars indicate stdev of measurements performed with three replicates.

Full-size DOI: 10.7717/peerj.10373/fig-1

a.

SIL, IC50 values					Rank of cell lines				
H1650	H1975	A549	H838	H2030	H1650	H1975	A549	H838	H2030
0,56	1,00	0,86	0,00	0,71	4	1	2	5	3

b.

WFA, IC50 values					Rank of cell lines				
H1650	H1975	A549	H838	H2030	H1650	H1975	A549	H838	H2030
0,00	0,18	0,44	0,35	1,00	5	4	2	3	1

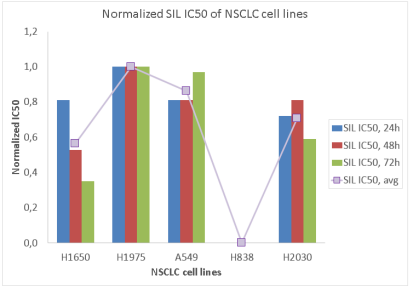

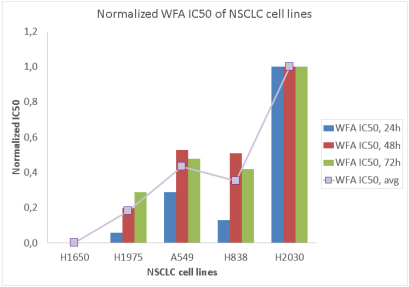

Figure 2 **Normalized 24 h, 48 h, 72 h and average IC50 of five NSCLC cell lines: (A) Silibinin, (B) Withaferin-A.**

Full-size DOI: 10.7717/peerj.10373/fig-2

and the EMT 58 gene signature from *Byers et al. (2013)* was calculated. From analysis of correlations between expression of 58 EMT genes and the pattern of SIL/WFA IC50 response, it follows that the WFA IC50 of NSCLC cells exhibits a significantly higher correlation with the EMT stage than the SIL IC50 response, see Table S1. Examples of significant WFA and poor SIL correlations with two major biomarkers of EMT (e.g., *CDH1* and *ZEB1*) are shown in Fig. 3. While gradient of WFA IC50 values from epithelial to mesenchymal cell lines is consistent with previous observations of elevated drug-resistance and survival potential of mesenchymal cells (*Tan et al., 2014*), low correlation of SIL IC50 with EMT gene expression (GE) appear to contradict this prevailing view.

In order to dissect further possible genes correlating with the pattern of SIL IC50 among five NSCLC cell lines, correlation analysis was performed at the whole genome scale under consideration of reliability of transcriptomic signals (i.e., M/P accepted, A excluded), see Table S2. From this analysis 144 genes with a positive correlation and significance level of $p < 0.05$ were identified. Gene ontology (GO) analysis of 144 genes positively correlating with the SIL IC50 signature of five NSCLC cell lines shows a significant enrichment in GO categories related to cell cycle, G2/M transition, nuclear localization, DNA-replication and repair, and related signaling and metabolic processes and functions, see Table S2. Furthermore, a statistically significant overlap between this group of 144 genes and 90 'high-communicability' genes from our previous pan-cancer analysis study (*Gladilin & Eils, 2017*) was detected (12/90=13.3 %, $p < 0.001$ hypergeometric test: hgt(22277, 144, 90, 12) = 5.7e−13), see Table S3. Notably, this set of 12 cell cycle process related genes includes three genes that are known to be prominent targets of *STAT3* transcription factor: *BIRC5* (*Alvarez & Frank, 2004*; *Gritsko et al., 2006*; *Carpenter & Lo, 2014*), *FOXM1* (*Mencalha et al., 2012*), *BRCA1* (*Snyder, Huang & Zhang, 2007*), see Fig. 4. Figure 5 shows correlation

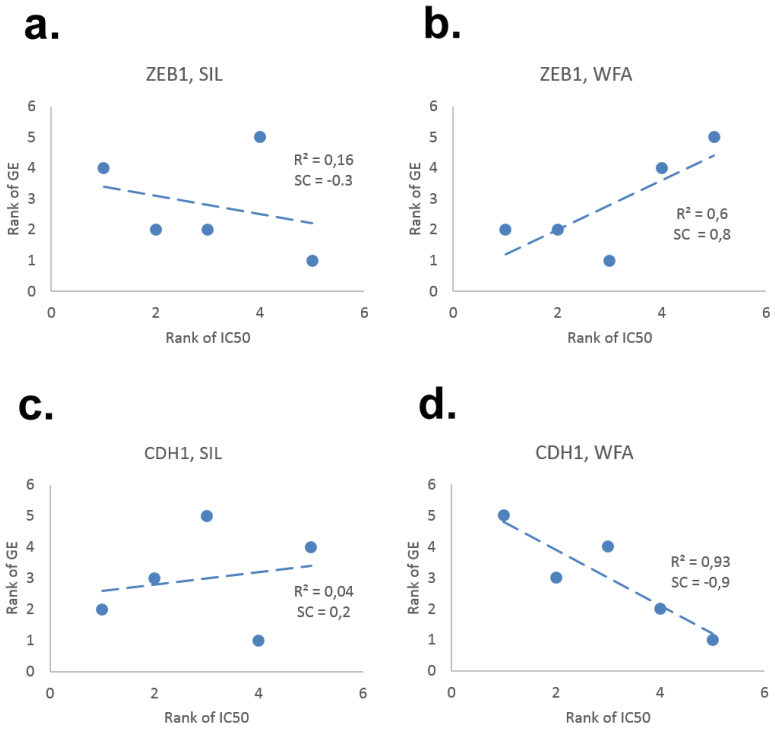

Figure 3 Examples of correlation between expression of (A, B) mesenchymal (*ZEB1*) and (C,D) epithelial (*CDH1*) genes with SIL/WFA IC50 in five NSCLC cell lines. While WFA IC50 strongly correlates with the pattern of EMT gene expression in NSCLC cells, SIL IC50 does not show any significant correlation with EMT genes; see details in Table S1.

Full-size DOI: 10.7717/peerj.10373/fig-3

between gene expression patterns of these three *STAT3* target genes and SIL IC50 response of five NSCLC cells vs. another three non-significantly correlating genes.

To evaluate the relevancy of computationally selected genes to SIL viability response of NSCLC cells, transient knockdown of *BIRC5*, *FOXM1*, *BRCA1* genes was performed. Even though the reverse transfection method was considered to be more efficient providing higher transfection rates with minimal nucleic acid usage (*Erfle et al., 2007*), here we found out forward transfection to show a better performance crossover five tested NSCLC cell lines, see Fig. S1. Reverse and forward transfection of siRNA targeting PLK1 resulted in the comparable phenotype frequencies in all tested cell lines. A459 and H838 responded strongly in both methods, whereas, H1650 and H2030 showed no phenotype. This may be attributed either to difficulties in transfecting these cells or non-responsiveness to PLK1 depletion. Nearly 50% of H1975 cells showed prometaphase arrest when using forward transfection, but hardly any effect was observed under the conditions of reverse transfection. Consequently, the forward transfection protocol was used for transfection of H1975, A549, H838 cells with target siRNA.

Comparative viability measurements of H1975, A549, H838 cells with transiently knocked down *BIRC5*, *FOXM1*, *BRCA1* genes confirmed their relevancy to SIL response with exception of *BIRC5* knockdown in H838 cells, see Fig. 6. We draw the negative result

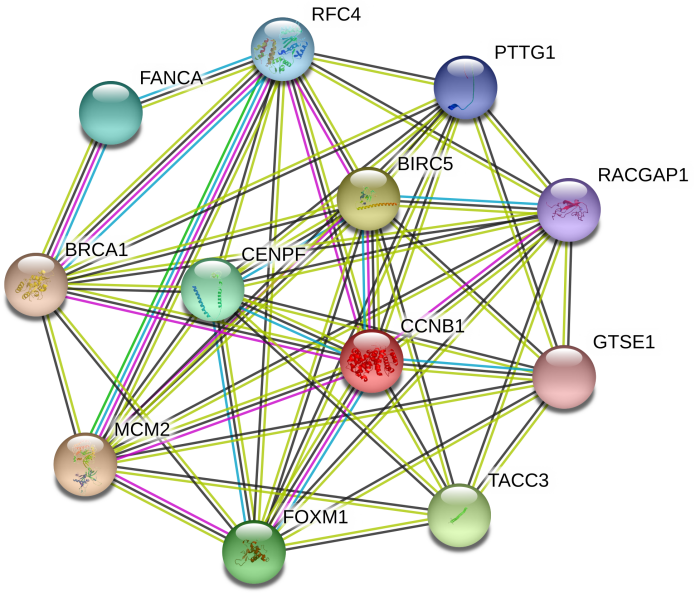

Figure 4 **Visualization of a subnetwork of tightly interconnected 12 genes from the overlap between the groups of 144 SIL-response relevant genes in five NSCLC cell lines and 90 high-communicability pan-cancer genes from (*Gladilin & Eils, 2017*) including three prominent targets of the *STAT3* transcription factor: *BIRC5*, *FOXM1*, *BRCA1* using STRING v11 (*Szklarczyk et al., 2019*) with default settings.**

Full-size DOI: 10.7717/peerj.10373/fig-4

of *BIRC5* knockdown in H838 cells back to constitutively low level of *BIRC5* in H838 in comparison to H1975, A549 cell lines. The relative changes in SIL response between control and knocked down NSCNC cells observed in this work are in the order of magnitude comparable with previous observations for other small weight compounds and NSCLC cell lines (*Gao et al., 2020*).

DISCUSSION

There is abundant evidence that Silibinin exhibits remarkable antineoplastic effects crossover different cancer tissue/cell types by affecting multiple molecular targets and pathways. However, not much is known about factors responsible for individual SIL viability response of cancer cells. Here, we systematically analyzed the relationship between the patterns of SIL IC50 and gene expression in five NSCLC cell lines exhibiting gradual difference with respect to their intrinsic EMT stage and compared it with the reference compound Withaferin-A. Our experimental results showed that, differently from WFA and other drugs, sensitivity of NSCLC cells to Silibinin does not correlate with the intrinsic EMT stage. Instead, a subset of cell cycle, survival and stress responsive genes including three prominent targets of *STAT3* (i.e., *BIRC5*, *FOXM1*, *BRCA1*) was found to exhibit significant correlation with the pattern of SIL IC50 in five NSCLC cell lines, see Fig. 7A. Subsequent evaluation of SIL viability response of transiently *BIRC5*, *FOXM1*, *BRCA1* silenced NSCLC cells confirmed computationally predicted dependency of SIL dose on the expression level of these genes. Since the expression of *STAT3* transcriptional targets but not *STAT3* itself

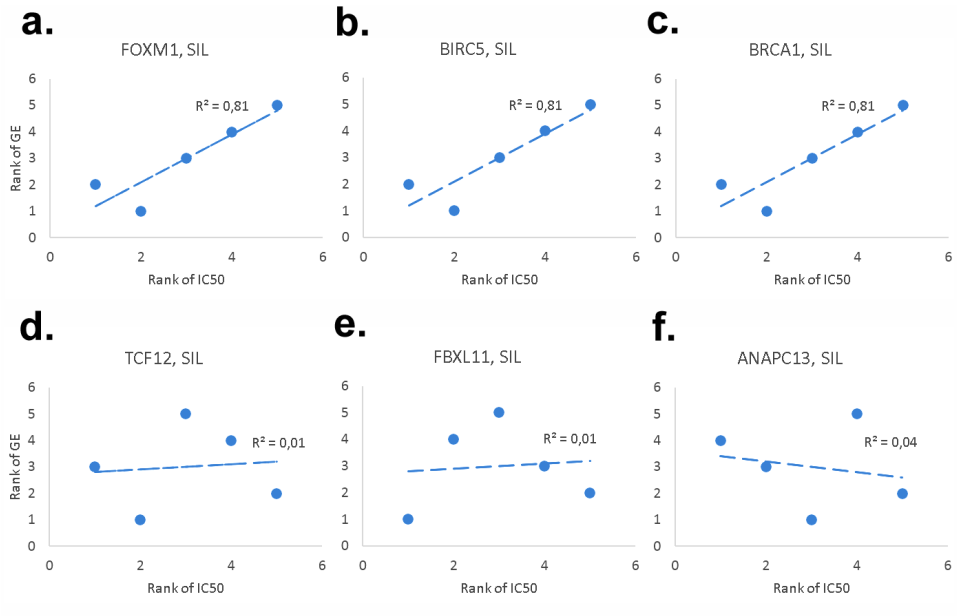

Figure 5 **Examples of genes with significant (*FOXM1* (A), *BIRC5* (B), *BRCA1* (C)) and non-significant (*TCF12* (D), *FBXL11* (E), *ANAPC13* (F)) correlation between the patterns of gene expression and normalized SIL IC50 in five NSCLC cell lines.**

Full-size DOI: 10.7717/peerj.10373/fig-5

significantly correlates with SIL IC50 of five NSCLC cell lines, we conclude that external and/or constitutive activation of *STAT3*, for example, due to gain-of-function mutations or enhanced upstream signaling (e.g., tyrosine kinase receptors, G protein coupled receptors, toll-like receptors, growth factor receptors) is responsible for differences in SIL sensitivity between different NSCLC cell lines, see Fig. 7B. In this point, our study confirms previous findings that inhibition *STAT3* and its downstream targets is one of the major mechanisms of Silibin antineoplastic action. Furthermore, our observations confirm previous findings that expression of known drug targets does not necessarily exhibit a significant correlation with IC50 (*Parca et al., 2019*), and that downstream targets of those drug targets may instead represent a more reliable reference for IC50 correlation studies.

Our correlation analysis between viability and whole trascriptome profiles of five NSCLC cell lines provides a rich source of information for further investigation of anti-neoplastic and EMT-inhibiting effects of Silibinin in cancer cells. Among the group of 144 proteins whose expression positively correlates with the SIL IC50 there are also significantly enriched ontological categories related to cytoskeleton regulation and organization, see Table S2. Our previous studies (*Gladilin, 2015*) indicated remarkable inhibiting effects of Silibinin on cancer cell migration and overall reorganization of vimentin and actin networks (Supplementary Figs. S2 and S3) that can be attributed to these cytoskeleton-related genes, see Fig. S4. While GO enrichment in this work was performed using conventional statistical testing, rapidly evolving deep learning techniques (e.g., *Cao et al., 2018*; *Le et al., 2019*) hold the promise of proving more in-depth insights into large gene expression and cell viability data in the future.

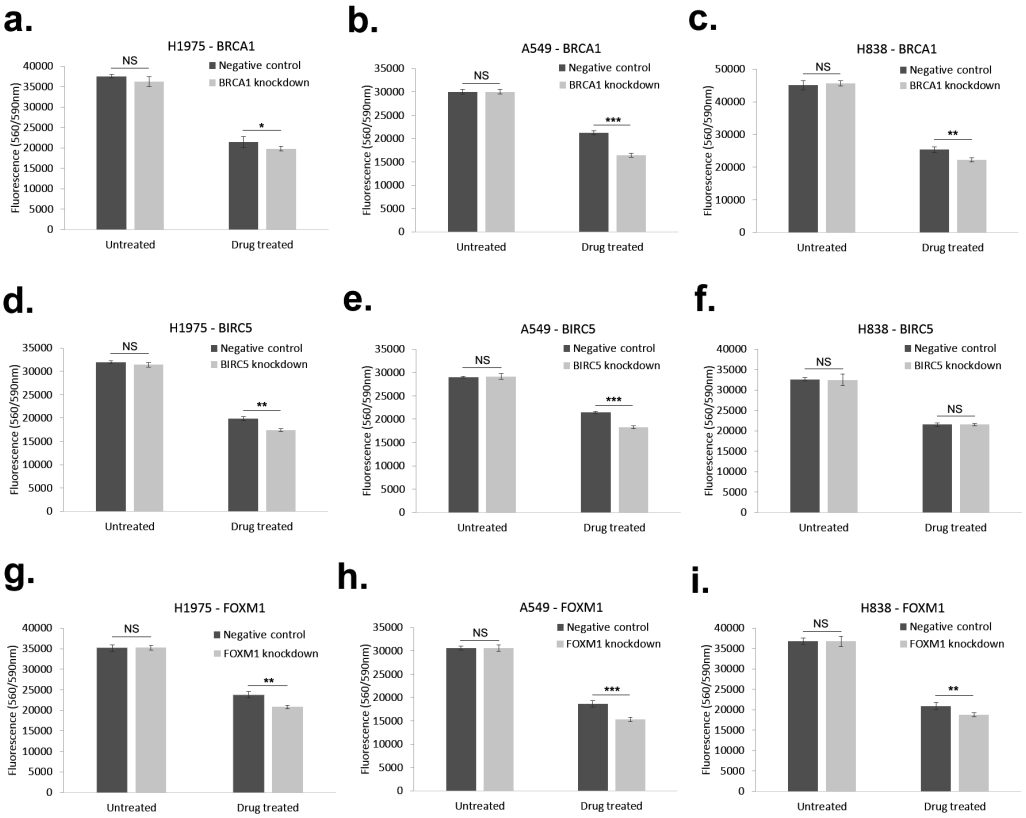

Figure 6 Summary of cell viability measurements of BRCA1 (A–C), BIRC5 (D–F) and FOXM1 (G–I) knocked down NSCLC cell lines with and without Silibinin treatment of H1975 (A, D, G), A549 (B, E, H) and H838 (C, F, I) NSCLC cell lines (see Table S4 for raw data for these plots). Error bars indicate stdev of measurements performed with three replicates. Negative control = NSCLC cells + lipofectamine® 2000 + scramble siRNA, knockdown = NSCLC cells + lipofectamine® 2000 + siRNA. NS, $p > 0.05$ (non-significant); *, $p < 0.05$; **, $p < 0.01$; ***, $p < 0.001$.

Full-size DOI: 10.7717/peerj.10373/fig-6

Furthermore, our experimental results suggest that the intrinsic EMT stage is not a suitable biomarker of SIL dose response of cancer cells. Instead, the subset of SIL IC50 correlating genes determined in this work can be used for dose optimization in adjuvant tumor therapy using Silibinin. Further investigations with a broader spectrum of NSCLC cells and other cancer cell lines are required to generalize preliminary findings of this study.

CONCLUSION

Silibinin inhibits NSCLC cell viability and motility in a dose-dependent manner. Thereby, SIL IC50 of different NSCLC cells does not correlate with their transcriptomic EMT signature. Instead, it was found that SIL dose–response correlates with the expression level of a network of 144 cell cycles, stress responsive and survival proteins including some well known targets of *STAT3*. It was shown that selected downstream targets of *STAT3* including *BRCA1*, *BIRC5*, *FOXM1* have impact on Silibinin dose response.

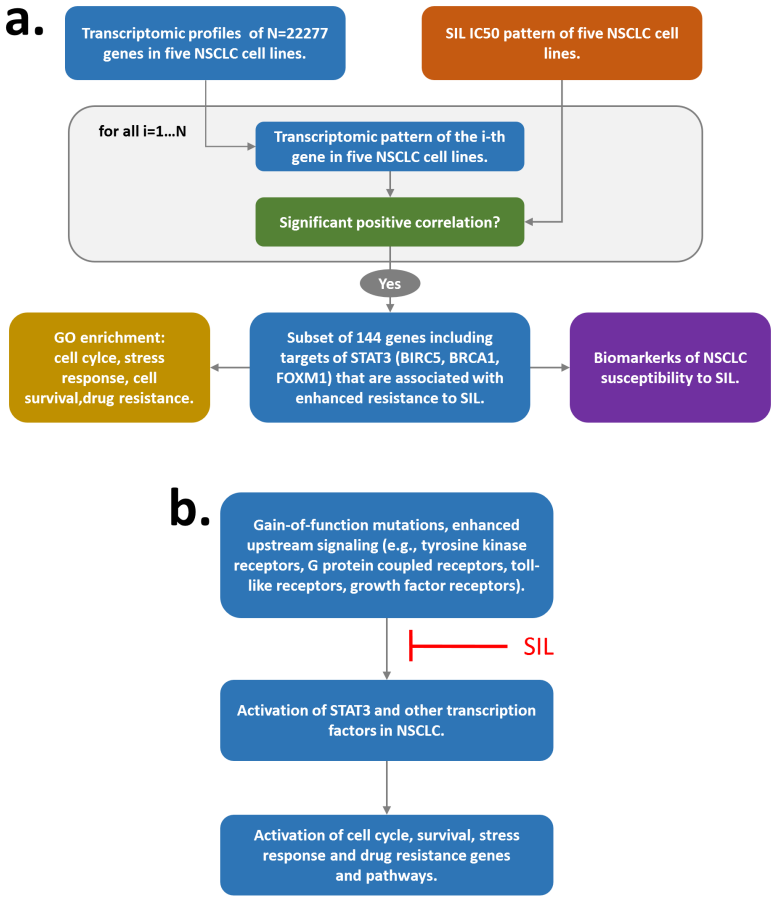

Figure 7 **Overall scheme of the study (A) and mechanistic explanation of experimental results (B).**
Full-size DOI: 10.7717/peerj.10373/fig-7

ACKNOWLEDGEMENTS

The authors are grateful to Dr. Marco Binder and Jürgen Beneke for helping with optimization and implementation of transfection assays, and to Katharina Jechow and Ellen Wiedtke for their support in cell culturing and microscopic imaging.

ADDITIONAL INFORMATION AND DECLARATIONS

Funding

Jagan Mohan Kaipa was supported by the DKFZ-MOST Grant c-160. The funders had no role in study design, data collection and analysis, decision to publish, or preparation of the manuscript.

Grant Disclosures

The following grant information was disclosed by the authors:
DKFZ-MOST: c-160.

Competing Interests

The authors declare there are no competing interests.

Author Contributions

- Jagan Mohan Kaipa and Evgeny Gladilin conceived and designed the experiments, performed the experiments, analyzed the data, prepared figures and/or tables, authored or reviewed drafts of the paper, and approved the final draft.
- Vytaute Starkuviene conceived and designed the experiments, analyzed the data, authored or reviewed drafts of the paper, and approved the final draft.
- Holger Erfle and Roland Eils conceived and designed the experiments, authored or reviewed drafts of the paper, and approved the final draft.

Data Availability

The following information was supplied regarding data availability:

The raw data are available in Tables S1–S4.

Supplemental Information

Supplemental information for this article can be found online at http://dx.doi.org/10.7717/peerj.10373#supplemental-information.

REFERENCES

Agarwal C, Singh RP, Dhanalakshmi S, Tyagi AK, Tecklenburg M, Sclafani RA, Agarwal R. 2003. Silibinin upregulates the expression of cyclin-dependent kinase inhibitors and causes cell cycle arrest and apoptosis in human colon carcinoma HT-29 cells. *Oncogene* **22(51)**:8271–8282 DOI 10.1038/sj.onc.1207158.

Agarwal C, Tyagi A, Kaur M, Agarwal R. 2007. Silibinin inhibits constitutive activation of Stat3, and causes caspase activation and apoptotic death of human prostate carcinoma DU145 cells. *Carcinogenesis* **28(7)**:1463–1470 DOI 10.1093/carcin/bgm042.

Al-Lazikani B, Banerji U, Workman P. 2012. Combinatorial drug therapy for cancer in the post-genomic era. *Nature Biotechnology* **30**:679–692 DOI 10.1038/nbt.2284.

Alvarez J, Frank D. 2004. Genome-wide analysis of STAT target genes: elucidating the mechanism of STAT-mediated oncogenesis. *Cancer Biology & Therapy* **3(11)**:1045–1050 DOI 10.4161/cbt.3.11.1172.

Bai Z-L, Tay V, Guo S-Z, Ren J, Shu M-G. 2018. Silibinin induced human glioblastoma cell apoptosis concomitant with autophagy through simultaneous inhibition of mTOR and YAP. *BioMed Research International* **2018**:6165192 DOI 10.1155/2018/6165192.

Beckmann-Knopp S, Rietbrock S, Weyhenmeyer R, Böcker R, Beckurts K, Lang W, Hunz M, Fuhr U. 2000. Inhibitory effects of silibinin on cytochrome P-450 enzymes in human liver microsomes. *Pharmacology and Toxicology* **86(6)**:250–256 DOI 10.1111/j.0901-9928.2000.860602.x.

Benyamini Y, Hochberg Y. 1995. Controlling the false discovery rate: a practical and powerful approach to multiple testin. *Journal of the Royal Statistical Society. Series B (Methodological)* **57**:289–300.

Bijak M. 2017. Silybin, a major bioactive component of milk thistle (*Silybum marianum* L. Gaernt.)—chemistry, bioavailability, and metabolism. *Molecules* **22(11)**:1942 DOI 10.3390/molecules22111942.

Bosch-Barrera J, Menendez JA. 2015. Silibinin and STAT3: a natural way of targeting transcription factors for cancer therapy. *Cancer Treatment Reviews* **41(6)**:540–546 DOI 10.1016/j.ctrv.2015.04.008.

Bosch-Barrera J, Queralt B, Menedez J. 2017. Targeting STAT3 with silibinin to improve cancer therapeutics. *Cancer Treatment Reviews* **58**:61–69 DOI 10.1016/j.ctrv.2017.06.003.

Byers L, Diao L, Wang J, Saintigny P, Girard L, Peyton M, Shen L, Fan Y, Giri U, Tumula P, Nilsson M, Gudikote J, Tran H, Cardnell R, Bearss D, Warner S, Foulks J, Kanner S, Gandhi V, Krett N, Rosen S, Kim E, Herbst R, Blumenschein G, Lee J, Lippman S, Ang K, Mills G, Hong W, Weinstein J, Wistuba II, Coombes K, Minna J, Heymach J. 2013. An epithelial-mesenchymal transition gene signature predicts resistance to EGFR and PI3K inhibitors and identifies Axl as a therapeutic target for overcoming EGFR inhibitor resistance. *Clinical Cancer Research* **19(1)**:279–290 DOI 10.1158/1078-0432.CCR-12-1558.

Byun H, Darvin P, Kang D, Sp N, Joung Y, Park J, Kim S, Yang Y. 2017. Silibinin down-regulates MMP2 expression via Jak2/STAT3 pathway and inhibits the migration and invasive potential in MDA-MB-231 cells. *Oncology Reports* **37(6)**:3270–3278 DOI 10.3892/or.2017.5588.

Cao C, Liu F, Tan H, Song D, Shu W, Li W, Zhou X, Bo X, Xi Z. 2018. Deep learning and its applications in biomedicine. *Genomics Proteomics Bioinformatics* **16(1)**:17–32 DOI 10.1016/j.gpb.2017.07.003.

Carpenter R, Lo H-W. 2014. STAT3 target genes relevant to human cancers. *Cancer* **6**:897–925 DOI 10.3390/cancers6020897.

Catanzaro D, Gabbia D, Cocetta V, Biagi M, Ragazzi E, Montopoli M, Carrara M. 2018. Silybin counteracts doxorubicin resistance by inhibiting GLUT1 expression. *Fitoterapia* **124**:42–48 DOI 10.1016/j.fitote.2017.10.007.

Chandarlapaty S, Scaltriti M, Angelini P, Ye Q, Guzman M, Hudis C, Norton L, Solit D, Arribas J, Baselga J, Rosen N. 2010. Inhibitors of HSP90 block p95-HER2 signaling in Trastuzumab-resistant tumors and suppress their growth. *Oncogene* **29(3)**:325–334 DOI 10.1038/onc.2009.337.

Chen Y-H, Chen C-L, Liang C-M, Liang J-B, Tai M-C, Chang Y-H, Lu D-W, Chen J-T. 2014. Silibinin inhibits ICAM-1 expression via regulation of N-linked and O-linked glycosylation in ARPE-19 cells. *BioMed Research International* **2014**:701395.

Chen P-N, Hsieh Y-S, Chiou H-L, Chu S-C. 2005. Silibinin inhibits cell invasion through inactivation of both PI3K-Akt and MAPK signaling pathways. *Chemico-Biological Interactions* **156(2–3)**:141–150 DOI 10.1016/j.cbi.2005.08.005.

Chinthakunta N, Cheemanapalli S, Chinthakunta S, Anuradha C, Chitta C. 2018. A new insight into identification of in silico analysis of natural compounds targeting GPR120. *Network Modeling and Analysis in Health Informatics and Bioinformatics Journal* **7**:8 DOI 10.1007/s13721-018-0166-0.

Chittezhath M, Deep G, Singh R, Agarwal C. 2008. Silibinin inhibits cytokine-induced signaling cascades and down-regulates inducible nitric oxide synthase in human lung carcinoma A549 cells. *Molecular Cancer Therapeutics* **7(7)**:1817–1826 DOI 10.1158/1535-7163.MCT-08-0256.

Clarke P, Roe T, Swabey K, Hobbs S, McAndrew C, Tomlin K, Westwood I, Burke R, Van Montfort R, Workman P. 2019. Dissecting mechanisms of resistance to targeted drug combination therapy in human colorectal cancer. *Oncogene* **38**:5076–5090 DOI 10.1038/s41388-019-0780-z.

Cufí S, Bonavia R, Vazquez-Martin A, Corominas-Faja B, Oliveras-Ferraros C, Cuyàs E, Martin-Castillo B, Barrajón-Catalán E, Visa J, Segura-Carretero A, Bosch-Barrera J, Joven J, Micol V, Menendez JA. 2013. Silibinin meglumine, a water-soluble form of milk thistle silymarin, is an orally active anti-cancer agent that impedes the epithelial-to-mesenchymal transition (EMT) in EGFR-mutant non-small-cell lung carcinoma cells. *Food and Chemical Toxicology* **60**:360–368 DOI 10.1016/j.fct.2013.07.063.

Cuyás E, Verdura S, Micol V, Joven J, Bosch-Barrera J, Encinar J, Menendez J. 2019. Revisiting silibinin as a novobiocin-like Hsp90 C-terminal inhibitor: computational modeling and experimental validation. *Food and Chemical Toxicology* **132**:110645 DOI 10.1016/j.fct.2019.110645.

Dastpeyman M, Motamed N, Azadmanesh K, Mostafavi E, Kia V, Jahanian-Najafabadi A, Shokrgozar MA. 2012. Inhibition of silibinin on migration and adhesion capacity of human highly metastatic breast cancer cell line, MDA-MB-231, by evaluation of β1-integrin and downstream molecules, Cdc42, Raf-1 and D4GDI. *Medical Oncology* **29(4)**:2512–2518 DOI 10.1007/s12032-011-0113-8.

Davis-Searles P, Nakanishi Y, Kim N, Graf T, Oberlies N, Wani M, Wall M, Agarwal R, Kroll D. 2005. Milk thistle and prostate cancer: differential effects of pure flavonolignans from Silybum marianum on antiproliferative end points in human prostate carcinoma cells. *Cancer Research* **65(10)**:4448–4457 DOI 10.1158/0008-5472.CAN-04-4662.

Dayem A, Choi H, Yang G, Kim K, Saha S, Cho S. 2016. The anti-cancer effect of polyphenols against breast cancer and cancer stem cells: molecular mechanisms. *Nutrients* **8**:581 DOI 10.3390/nu8090581.

Deep G, Singh RP, Agarwal C, Kroll DJ, Agarwal R. 2006. Silymarin and silibinin cause G1 and G2-M cell cycle arrest via distinct circuitries in human prostate cancer PC3 cells: a comparison of flavanone silibinin with flavanolignan mixture silymarin. *Oncogene* **25**:1053–1069 DOI 10.1038/sj.onc.1209146.

Dhanalakshmi S, Mallikarjuna G, Singh R, Agarwal R. 2004. Silibinin prevents ultraviolet radiation-caused skin damages in SKH-1 hairless mice via a decrease in thymine dimer positive cells and an up-regulation of p53-p21/Cip1 in epidermis. *Carcinogenesis* **25**:1459–1465 DOI 10.1093/carcin/bgh152.

El-Chaar N, Piccolo S, Boucher K, Cohen A, Chang J, Moos P, Bild A. 2014. Genomic classification of the RAS network identifies a personalized treatment strategy for lung cancer. *Molecular Oncology* **8(7)**:1339–1354 DOI 10.1016/j.molonc.2014.05.005.

Erfle H, Neumann B, Liebel U, Rogers P, Held M, Walter T, Pepperkok R. 2007. Reverse transfection on cell arrays for high content screening microscopy. *Nature Protocols* **2(2)**:392–399 DOI 10.1038/nprot.2006.483.

Fan S, Li L, Chen S, Yu Y, Qi M, Tashiro S, Onodera S, Ikejima T. 2011. Silibinin induced-autophagic and apoptotic death is associated with an increase in reactive oxygen and nitrogen species in hela cells. *Free Radical Research* **45**:1307–1324 DOI 10.3109/10715762.2011.618186.

Flora K, Hahn M, Rosen H, Benner K. 1998. Milk thistle (Silybum marianum) for the therapy of liver disease. *The American Journal of Gastroenterology* **93(2)**:139–143 DOI 10.1111/j.1572-0241.1998.00139.x.

Fraschini F, Demartini G, Esposti D. 2002. Pharmacology of silymarin. *Clinical Drug Investigation* **22(15)**:51–65 DOI 10.2165/00044011-200222010-00007.

Gao F, Yu X, Li M, Zhou L, Liu W, Li W, Lio H. 2020. Deguelin suppresses non-small cell lung cancer by inhibiting EGFR signaling and promoting GSK3β/FBW7-mediated Mcl-1 destabilization. *Cell Death & Disease* **11**:143 DOI 10.1038/s41419-020-2344-0.

García-Maceira P, Mateo J. 2009. Silibinin inhibits hypoxia-inducible factor-1alpha and mTOR/p70S6K/4E-BP1 signalling pathway in human cervical and hepatoma cancer cells: implications for anticancer therapy. *Oncogene* **28**:313–324 DOI 10.1038/onc.2008.398.

Gazak R, Walterova D, Kren V. 2007. Silybin and silymarin—new and emerging applications in medicine. *Current Medicinal Chemistry* **14(3)**:315–338 DOI 10.2174/092986707779941159.

Gerhäuser C. 2012. Cancer cell metabolism, epigenetics and the potential influence of dietary components—a perspective. *Biomedical Research* **23(1)**:561–567.

Gladilin E. 2015. Dissecting antineoplastic effects of EMT-reverting phytocompounds Silibinin and Withaferin-A. In: *Third annual broad-ISF symposium on cell circuits, Konrad Adenauer Conference Center, Jerusalem, Israel, June 8–10.*

Gladilin E, Eils R. 2017. Graph-theoretical model of global human interactome reveals enhanced long-range communicability in cancer networks. *PLOS ONE* **12**:e0170953 DOI 10.1371/journal.pone.0170953.

Gladilin E, Gonzalez P, Eils R. 2014. Dissecting the contribution of actin and vimentin intermediate filaments to mechanical phenotype of suspended cells using high-throughput deformability measurements and computational modeling. *Journal of Biomechanics* **47(11)**:2598–2605 DOI 10.1016/j.jbiomech.2014.05.020.

Gritsko T, Williams A, Turkson J, Kaneko S, Bowman T, Huang M, Nam S, Eweis I, Diaz N, Sullivan D, Yoder S, Enkemann S, Eschrich S, Lee J, Beam C, Cheng J, Minton S, Muro-Cacho C, Jove R. 2006. Persistent activation of Stat3 signaling induces survivin gene expression and confers resistance to apoptosis in human breast cancer cells. *Clinical Cancer Research* **12(1)**:11–19 DOI 10.1158/1078-0432.CCR-04-1752.

Hanahan D, Weinberg R. 2011. Hallmarks of cancer: the next generation. *Cell* **144(5)**:646–674 DOI 10.1016/j.cell.2011.02.013.

Hang Y, Cai X, Fan D. 2013. Roles of epithelial-mesenchymal transition in cancer drug resistance. *Current Cancer Drug Targets* **13**:915–929 DOI 10.2174/15680096113136660097.

Hellerbrand C, Schattenberg J, Peterburs P, Lechner A, Brignoli R. 2016. The potential of silymarin for the treatment of hepatic disorders. *Clinical Phytoscience* **2**:7.

Hosen S, Kabir M, Hasanat A, Chowdhury T, Chakrabarty N, Sarker S, Kader S, MR H, Dash R. 2016. Docking and ADME/T analysis of silibinin as a potential inhibitor of EGFR kinase for ovarian cancer therapy. *Journal of Applied Pharmaceutical Science* **6(08)**:001–005.

Hou X, Du H, Quan X, Shi L, Zhang Q, Wu Y, Liu Y, Xiao J, Li Y, Lu L, Ai X, Zhan M, Yuan S, Sun L. 2018. Silibinin inhibits NSCLC metastasis by targeting the EGFR/LOX pathway. *Frontiers in Pharmacology* **9**:21 DOI 10.3389/fphar.2018.00021.

Housman G, Byler S, Heerboth S, Lapinska K, Longacre M, Snyder N, Sarkar S. 2014. Drug resistance in cancer: an overview. *Cancers* **6(3)**:1769–1792 DOI 10.3390/cancers6031769.

Iftikhar H, Rashid S. 2014. Molecular docking studies of flavonoids for their inhibition pattern against β-catenin and pharmacophore model generation from experimentally known flavonoids to fabricate more potent inhibitors for Wnt signaling pathway. *Pharmacognosy Magazine* **10(Suppl 2)**:S264–S271 DOI 10.4103/0973-1296.133269.

Jiang K, Wang W, Jin X, Wang Z, Ji Z, Meng G. 2015. Silibinin, a natural flavonoid, induces autophagy via ROS-dependent mitochondrial dysfunction and loss of ATP involving BNIP3 in human MCF7 breast cancer cells. *Oncology Reports* **33(6)**:2711–2718 DOI 10.3892/or.2015.3915.

Kang JS, Park S-K, Yang K-H, Kim HM. 2003. Silymarin inhibits TNF- α-induced expression of adhesion molecules in human umbilical vein endothelial cells. *FEBS Letters* **550(1–3)**:89–93 DOI 10.1016/S0014-5793(03)00827-5.

Katiyar SK, Roy AM, Baliga MS. 2005. Silymarin induces apoptosis primarily through a p53-dependent pathway involving Bcl-2/Bax, cytochrome c release, and caspase activation. *Molecular Cancer Therapeutics* **4(February)**:207–216.

Kauntz H. 2012. Cellular and molecular targets of silibinin, a natural flavonoid, in colorectal cancer prevention and therapy. *PhD thesis, University of Strasbourg, Strasbourg, France. Available at https://tel.archives-ouvertes.fr/tel-00768301*.

Kauntz H, Bousserouel S, Gosse F, Marescaux J, Raul F. 2012. Silibinin, a natural flavonoid, modulates the early expression of chemoprevention biomarkers in a preclinical model of colon carcinogenesis. *International Journal of Oncology* **41(3)**:849–854 DOI 10.3892/ijo.2012.1526.

Kawaguchi-Suzuki M, Frye R, Zhu H, Brinda B, Chavin K, Bernstein H, Markowitz J. 2014. The effects of milk thistle (Silybum marianum) on human cytochrome P450 activity. *Drug Metabolism and Disposition: The Biological Fate of Chemicals* **42(10)**:1611–1616 DOI 10.1124/dmd.114.057232.

Kim S, Jeon M, Lee J, Han J, Oh S, Jung T, Nam S, Kil W, Lee J. 2014a. Induction of fibronectin in response to epidermal growth factor is suppressed by silibinin through

the inhibition of STAT3 in triple negative breast cancer cells. *Oncology Reports* **32(5)**:2230–2236 DOI 10.3892/or.2014.3450.

Kim TH, Woo JS, Kim YK, Kim KH. 2014b. Silibinin induces cell death through reactive oxygen species-dependent downregulation of notch-1/ERK/Akt signaling in human breast cancer cells. *The Journal of Pharmacology and Experimental Therapeutics* **349(2)**:268–278 DOI 10.1124/jpet.113.207563.

Le N, Yapp E, Nagasundaram N, Chua M, Yeh H. 2019. Computational identification of vesicular transport proteins from sequences using deep gated recurrent units architecture. *Computational and Structural Biotechnology Journal* **17**:1245–1254 DOI 10.1016/j.csbj.2019.09.005.

Lin M, Chien P, Wu H, Chen S, Juan H, Lou P, Huang M. 2018. C1GALT1 predicts poor prognosis and is a potential therapeutic target in head and neck cancer. *Oncogene* **37**:5780–5793 DOI 10.1038/s41388-018-0375-0.

Machicao F, Sonnenbichler J. 1977. Mechanism of the stimulation of RNA synthesis in rat liver nuclei by silybin. *Hoppe-Seyler's Zeitschrift für physiologische Chemie* **358(2)**:141–147 DOI 10.1515/bchm2.1977.358.1.141.

Malik A, Manan A, Kirza U. 2017. Molecular docking and in silico ADMET studies of silibinin and glycyrrhetic acid anti-inflammatory activity. *Tropical Journal of Pharmaceutical Research* **16(1)**:67–74 DOI 10.4314/tjpr.v16i1.9.

Manna S, Mukhopadhyay A, Van N, Aggarwal B. 1999. Silymarin suppresses TNF-induced activation of NF-kappa B, c-Jun N-terminal kinase, and apoptosis. *Journal of Immunology* **163(12)**:6800–6809.

Marwitz S, Depner S, Dvornikov D, Merkle R, Szczygieł M, Müller-Decker K, Lucarelli P, Wäsch M, Mairbäurl H, Rabe KF, Kugler C, Vollmer E, Reck M, Scheufele S, Kröger M, Ammerpohl O, Siebert R, Goldmann T, Klingmüller U. 2016. Downregulation of the TGFβ pseudoreceptor BAMBI in non-small cell lung cancer enhances TGFβ signaling and invasion. *Cancer Research* **76(13)**:3785–3801 DOI 10.1158/0008-5472.CAN-15-1326.

Mencalha A, Binato R, Ferreira G, Du Rocher B, Abdelhay E. 2012. Forkhead Box M1 (FoxM1) gene is a new STAT3 transcriptional factor target and is essential for proliferation, survival and DNA repair of K562 cell line. *PLOS ONE* **7(10)**:e48160 DOI 10.1371/journal.pone.0048160.

Michael M, Doherty M. 2005. Tumoral drug metabolism: overview and its implications for cancer therapy. *Journal of Clinical Oncology* **23**:205–229 DOI 10.1200/JCO.2005.02.120.

Mokhtari M, Motamed N, Shokrgozar M. 2008. Evaluation of silibinin on the viability, migration and adhesion of the human prostate adenocarcinoma (PC-3) cell line. *Cell Biology International* **32(8)**:888–892 DOI 10.1016/j.cellbi.2008.03.019.

Nambiar DK, Deep G, Singh RP, Agarwal C, Agarwal R. 2014. Silibinin inhibits aberrant lipid metabolism, proliferation and emergence of androgen-independence in prostate cancer cells via primarily targeting the sterol response element binding protein 1. *Oncotarget* **5(20)**:10017–10033 DOI 10.18632/oncotarget.2488.

Parca L, Pepe G, Pietrosanto M, Galvan G, Galli L, Palmeri A, Sciandrone M, Ferre F, Ausiello G, Helmer-Citterich M. 2019. Modeling cancer drug response through drug-specific informative genes. *Scientific Reports* **9**:15222 DOI 10.1038/s41598-019-50720-0.

Patel N, Rothenberg M. 1994. Multidrug resistance in cancer chemotherapy. *Investigational New Drugs* **12(1)**:1–13 DOI 10.1007/BF00873229.

Patel S, Waghela B, Shah K, Vaidya F, Mirza S, Patel S, Pathak C, Rawal R. 2018. Silibinin, A natural blend in polytherapy formulation for targeting Cd44v6 expressing colon cancer stem cells. *Scientific Reports* **8**:16985 DOI 10.1038/s41598-018-35069-0.

Pirouzpanah MB, Sabzichi M, Pirouzpanah S, Chavoshi H, Samadi N. 2015. Silibilin-induces apoptosis in breast cancer cells by modulating p53, p21, Bak and Bcl-XL pathways. *Asian Pacific Journal of Cancer Prevention* **16(5)**:2087–2092 DOI 10.7314/APJCP.2015.16.5.2087.

Polachi N, Bai G, Li T, Chu Y, Wang X, Li S, Gu N, Wu J, Li W, Zhang Y, Zhou S, Sun H, Liu C. 2016. Modulatory effects of silibinin in various cell signaling pathways against liver disorders and cancer—A comprehensive review. *European Journal of Medicinal Chemistry* **123**:577–595 DOI 10.1016/j.ejmech.2016.07.070.

Poór M, Boda G, Mohos V, Kuzma M, Bálint M, Hetényi C, Bencsik T. 2018. Pharmacokinetic interaction of diosmetin and silibinin with other drugs: inhibition of CYP2C9-mediated biotransformation and displacement from serum albumin. *Biomedicine and Pharmacotherapy* **102**:912–921 DOI 10.1016/j.biopha.2018.03.146.

Preibisch S, Saalfeld S, Tomancak P. 2009. Globally optimal stitching of tiled 3D microscopic image acquisitions. *Bioinformatics* **25(11)**:1463–1465 DOI 10.1093/bioinformatics/btp184.

Pubmed. 2019. List of Silibinin-related publications. *Available at https://www.ncbi.nlm.nih.gov/pubmed/?term=silibinin*.

Qin J, Yan L, Zhang J, Zhang W. 2019. STAT3 as a potential therapeutic target in triple negative breast cancer: a systematic review. *Journal of Experimental & Clinical Cancer Research* **38(1)**:195 DOI 10.1186/s13046-019-1206-z.

Raina K, Agarwal C, Wadhwa R, Serkova N, Agarwal R. 2013. Energy deprivation by silibinin in colorectal cancer cells: a double-edged sword targeting both apoptotic and autophagic machineries. *Autophagy* **9(5)**:697–713 DOI 10.4161/auto.23960.

Ramasamy K, Agarwal R. 2008. Multitargeted therapy of cancer by silymarin. *Cancer Letters* **269(2)**:352–362 DOI 10.1016/j.canlet.2008.03.053.

Riebold M, Kozany C, Freiburger L, Sattler M, Buchfelder M, Hausch F, Stalla GK, Paez-Pereda M. 2015. A C-terminal HSP90 inhibitor restores glucocorticoid sensitivity and relieves a mouse allograft model of Cushing disease. *Nature Medicine* **21(3)**:276–280.

Sebaugh J. 2011. Guidelines for accurate EC50/IC50 estimation. *Pharmaceutical Statistics* **10(2)**:128–134 DOI 10.1002/pst.426.

Shukla SK, Dasgupta A, Mehla K, Gunda V, Vernucci E, Souchek J, Goode G, King R, Mishra A, Rai I, Nagarajan S, Chaika NV, Yu F, Singh PK. 2015. Silibinin-mediated metabolic reprogramming attenuates pancreatic cancer-induced cachexia and tumor growth. *Oncotarget* **6(38)**:41146–41161 DOI 10.18632/oncotarget.5843.

Snyder M, Huang X-Y, Zhang J. 2007. Identification of novel direct STAT3 taget genes for control of growth and differentiation. *Journal of Biological Chemistry* **283(7)**:3791–3798.

Soleimani V, Delghandi P, Moallem S, Karimi G. 2019. Safety and toxicity of silymarin, the major constituent of milk thistle extract: an updated review. *Phytotherapy Research* **33(6)**:1627–1638 DOI 10.1002/ptr.6361.

Sonnenbichler J, Scalera F, Sonnenbichler I, Weyhenmeyer R. 1999. Stimulatory effects of silibinin and silicristin from the milk thistle Silybum marianum on kidney cells. *The Journal of Pharmacology and Experimental Therapeutics* **290(3)**:1375–1383.

Spiess A, Neumeyer N. 2010. An evaluation of R2 as an inadequate measure for nonlinear models in pharmacological and biochemical research: a Monte Carlo approach. *BMC Pharmacology* **10(1)**:6.

Su C-H, Chen L-J, Liao JF, Cheng J-T. 2013. Increase of phosphatase and tensin homolog by silymarin to inhibit human pharynx squamous cancer. *Journal of Medicinal Food* **16(9)**:778–784 DOI 10.1089/jmf.2012.2534.

Szklarczyk D, Gable A, Lyon D, Junge A, Wyder S, Huerta-Cepas J, Simonovic M, Doncheva N, Morris J, Bork P, Jensen L, Mering C. 2019. STRING v11: protein-protein association networks with increased coverage, supporting functional discovery in genome-wide experimental datasets. *Nucleic Acids Research* **47(D1)**:D607–D613 DOI 10.1093/nar/gky1131.

Tan T, Miow Q, Miki Y, Noda T, Mori S, Huang R, Thiery J. 2014. Epithelial-mesenchymal transition spectrum quantification and its efficacy in deciphering survival and drug responses of cancer patients. *EMBO Molecular Medicine* **6(10)**:1279–1293 DOI 10.15252/emmm.201404208.

Thomford N, Dzobo K, Chimusa E, Andrae-Marobela K, Chirikure S, Wonkam A, Dandara C. 2018. Personalized Herbal Medicine? A roadmap for convergence of herbal and precision medicine biomarker innovations. *OMICS* **22(6)**:375–391 DOI 10.1089/omi.2018.0074.

Ting H, Deep G, Agarwal R. 2013. Molecular mechanisms of silibinin-mediated cancer chemoprevention with major emphasis on prostate cancer. *The AAPS Journal* **15(3)**:707–716 DOI 10.1208/s12248-013-9486-2.

Tyagi A, Singh R, Ramasamy K, Raina K, Redente E, Dwyer-Nield L, Radcliffe R, Malkinson A, Agarwal R. 2009. Growth inhibition and regression of lung tumors by silibinin: modulation of angiogenesis by macrophage-associated cytokines and nuclear factor-κb and signal transducers and activators of transcription 3. *Cancer Prevention Research* **2**:74–83 DOI 10.1158/1940-6207.CAPR-08-0095.

Vanden Berghe W, Sabbe L, Kaileh M, Haegeman G, Heyninck K. 2012. Molecular insight in the multifunctional activities of Withaferin A. *Biochemical Pharmacology* **84(10)**:1282–1291 DOI 10.1016/j.bcp.2012.08.027.

Vargas-Mendoza N. 2014. Hepatoprotective effect of silymarin. *World Journal of Hepatology* **6(3)**:144–149 DOI 10.4254/wjh.v6.i3.144.

Verdura S, Cuyàs E, Llorach-Parés L, Pérez-Sánchez A, Micol V, Nonell-Canals A, Joven J, Valiente M, Sánchez-Martínez M, Bosch-Barrera J, Menendez J. 2018. Silibinin is a direct inhibitor of STAT3. *Food and Chemical Toxicology* **116**:161–172 DOI 10.1016/j.fct.2018.04.028.

Vyas AR, Singh SV. 2014. Molecular targets and mechanisms of cancer prevention and treatment by withaferin a, a naturally occurring steroidal lactone. *The AAPS Journal* **16(1)**:1–10 DOI 10.1208/s12248-013-9531-1.

Wang Y, Liang W-C, Pan W-L, Law W-K, Hu J-S, Ip DT-M, Waye MM-Y, Ng T-B, Wan DC-C. 2014a. Silibinin, a novel chemokine receptor type 4 antagonist, inhibits chemokine ligand 12-induced migration in breast cancer cells. *Phytomedicine* **21(11)**:1310–1317 DOI 10.1016/j.phymed.2014.06.018.

Wang Y-X, Cai H, Jiang G, Zhou T-B, Wu H. 2014b. Silibinin inhibits proliferation, induces apoptosis and causes cell cycle arrest in human gastric cancer MGC803 cells via STAT3 pathway inhibition. *Asian Pacific Journal of Cancer Prevention* **15(16)**:6791–6798 DOI 10.7314/APJCP.2014.15.16.6791.

Wang Z, Liu X, Ho R, Lam C, Chow M. 2016. Precision or personalized medicine for cancer chemotherapy: is there a role for herbal medicine. *Molecules* **21(7)**:889 DOI 10.3390/molecules21070889.

Wu K, Ning Z, Zeng J, Fan J, Zhou J, Zhang T, Zhang L, Chen Y, Gao Y, Wang B, Guo P, Li L, Wang X, He D. 2013. Silibinin inhibits β-catenin/ZEB1 signaling and suppresses bladder cancer metastasis via dual-blocking epithelial-mesenchymal transition and stemness. *Cellular Signalling* **25(12)**:2625–2633 DOI 10.1016/j.cellsig.2013.08.028.

Yoo H, Jung S, Hwang Y, Park J, Kim M, Jeong M, Ahn S, Ahn B, Shin B, Park R, Jung Y. 2004. Involvement of NF-kappaB and caspases in silibinin-induced apoptosis of endothelial cells. *International Journal of Molecular Medicine* **13**:81–86.

Youn CK, Park SJ, Lee MY, Cha MJ, Kim OH, You HJ, Chang IY, Yoon SP, Jeon YJ. 2013. Silibinin inhibits LPS-induced macrophage activation by blocking p38 MAPK in RAW 264.7 cells. *Biomolecules & Therapeutics* **21(4)**:258–263 DOI 10.4062/biomolther.2013.044.

Zhan T, Digel M, Küch EM, Stremmel W, Füllekrug J. 2011. Silybin and dehydrosilybin decrease glucose uptake by inhibiting GLUT proteins. *Journal of Cellular Biochemistry* **112(3)**:849–859 DOI 10.1002/jcb.22984.

Zhang M, Liu Y, Gao Y, Li S. 2015. Silibinin-induced glioma cell apoptosis by PI3K-mediated but Akt-independent downregulation of FoxM1 expression. *European Journal of Pharmacology* **765**:346–354 DOI 10.1016/j.ejphar.2015.08.057.

Zhao H, Brandt GE, Galam L, Matts RL, Blagg BSJ. 2011. Identification and initial SAR of silybin: an Hsp90 inhibitor. *Bioorganic & Medicinal Chemistry Letters* **21(9)**:2659–2664 DOI 10.1016/j.bmcl.2010.12.088.

Zheng N, Zhang P, Huang H, Liu W, Hayashi T, Zang L, Zhang Y, Liu L, Xia M, Tashiro S. 2015. Erα down-regulation plays a key role in silibinin-induced autophagy and

apoptosis in human breast cancer MCF-7 cells. *Journal of Pharmacological Sciences* **128**:97–107 DOI 10.1016/j.jphs.2015.05.001.

Zi X, Agarwal R. 1999. Silibinin decreases prostate-specific antigen with cell growth inhibition via G1 arrest, leading to differentiation of prostate carcinoma cells: implications for prostate cancer intervention. *Proceedings of the National Academy of Sciences of the United States of America* **96**(**13**):7490–7495 DOI 10.1073/pnas.96.13.7490.